Single-molecule displacement assay reveals strong binding of polyvalent dendrimer ligands to telomeric G-quadruplex

Pravin Pokhrel [a, †], Shogo Sasaki [b, †], Changpeng Hu [a, #], Deepak Karna [a], Shankar Pandey [a], Yue Ma [c], Kazuo Nagasawa [b], Hanbin Mao [a, *]

[a] Department of Chemistry and Biochemistry, Kent State University, Kent, OH 44242, USA

[b] Department of Biotechnology and Life Science Faculty of Technology, Tokyo University of Agriculture and Technology (TUAT), 2-14-16 Naka-cho, Koganeishi, Tokyo 184-8588, Japan

[c] Institute of Global Innovation Research, Tokyo University of Agriculture and Technology (TUAT), 2-14-16 Naka-cho, Koganeishi, Tokyo 184-8588, Japan

[#] Department of Pharmacy, The Second Affiliated Hospital, Army Medical University, Chongqing 400037, China

[†] These authors contributed equally.

* Author of correspondence.

Abstract

Binding between a ligand and a receptor is a fundamental step in many natural or synthetic processes. In biosensing, a tight binding with a small dissociation constant (K_d) between the probe and analyte can lead to superior specificity and sensitivity. Owing to their capability of evaluating competitors, displacement assays have been used to estimate K_d at the ensemble average level. At the more sensitive single-molecule level, displacement assays are yet to be established. Here, we developed a single-molecule displacement assay (smDA) in an optical tweezers instrument and used this innovation to evaluate the binding of the L2H2-6OTD ligands to human telomeric DNA G-quadruplexes. After measuring K_d of linear and dendrimer L2H2-6OTD ligands, we found that dendrimer ligands have enhanced binding affinity to the G-quadruplexes due to their polyvalent geometry. This increased binding affinity enhanced inhibition of telomerase elongation on a telomere template in a Telomerase Repeated Amplification Protocol (TRAP). Our experiments demonstrate that the smDA approach can efficiently evaluate binding processes in chemical and biological processes.

Keywords

Displacement assay, G-quadruplex, L2H2-6OTD, binding, single-molecule

1. Introduction

Molecular binding often serves as a first step in many chemical, biochemical, and biological processes. In organic reactions, binding of two reactants can determine the stereochemistry of products. In catalytic or enzymatic reactions, turnover of a substrate starts with its binding to the catalytic site. In cell signaling pathways, messenger molecules bind to receptors to elicit cell responses. Binding between a probe and an analyte constitutes the first step to determine the specificity and sensitivity of a (bio)sensing device. A tight binding with a small dissociation constant (K_d) between the probe and analyte often leads to high sensitivity since the analyte can bind to the probe even at low concentration levels.

To measure K_d, it is necessary to differentiate ligand-bound receptors from free receptors. This task can be achieved by heterogenous assays[1] in which bound and unbound species are physically separated. During the multi-step separation process which may occur in a prolonged period, uncertainty is introduced since receptors and ligands may become re-equilibrated. Alternatively, homogenous assays[1] can be carried out to differentiate ligand-free from ligand-bound receptors. In this approach, fluorescence or absorbance signals are often used in an ensemble average setting in which averaged signals compromise the sensitivity of the K_d measurement. To increase the sensitivity in the K_d determination, recently, single-molecule techniques have been used. As a particular example, single-molecule fluorescence resonance energy transfer (FRET) has been exploited to study the molecular binding between interactions of DNA-protein, DNA-ligand, protein-ligand, or protein-protein pairs.[2-7] While single-molecule fluorescence has superior mass sensitivity with respect to those performed at the ensemble average level, its signals can be compromised by background interference from environment. Force based single-molecule tools[8] such as atomic force microscopy (AFM),[9-15] optical tweezers,[16-20] and magnetic tweezers,[21-25] experience little force-related environmental interference. Recently, these force-based approaches have been used to measure K_d[26-28] as well as to serve as a new signal transduction means (mechanochemical transduction)[29] in biosensing.

When different species are present other than those of cognate binding components, few single-molecule approaches[30] exist to evaluate the K_d of the cognate binding process. In ensemble average assays, this task can be achieved by displacement assays in which receptors bound with one ligand are replaced by the same or different types of ligands.[31, 32] Such a method is efficient to evaluate ligands different from the cognate ligand. In addition, it simplifies

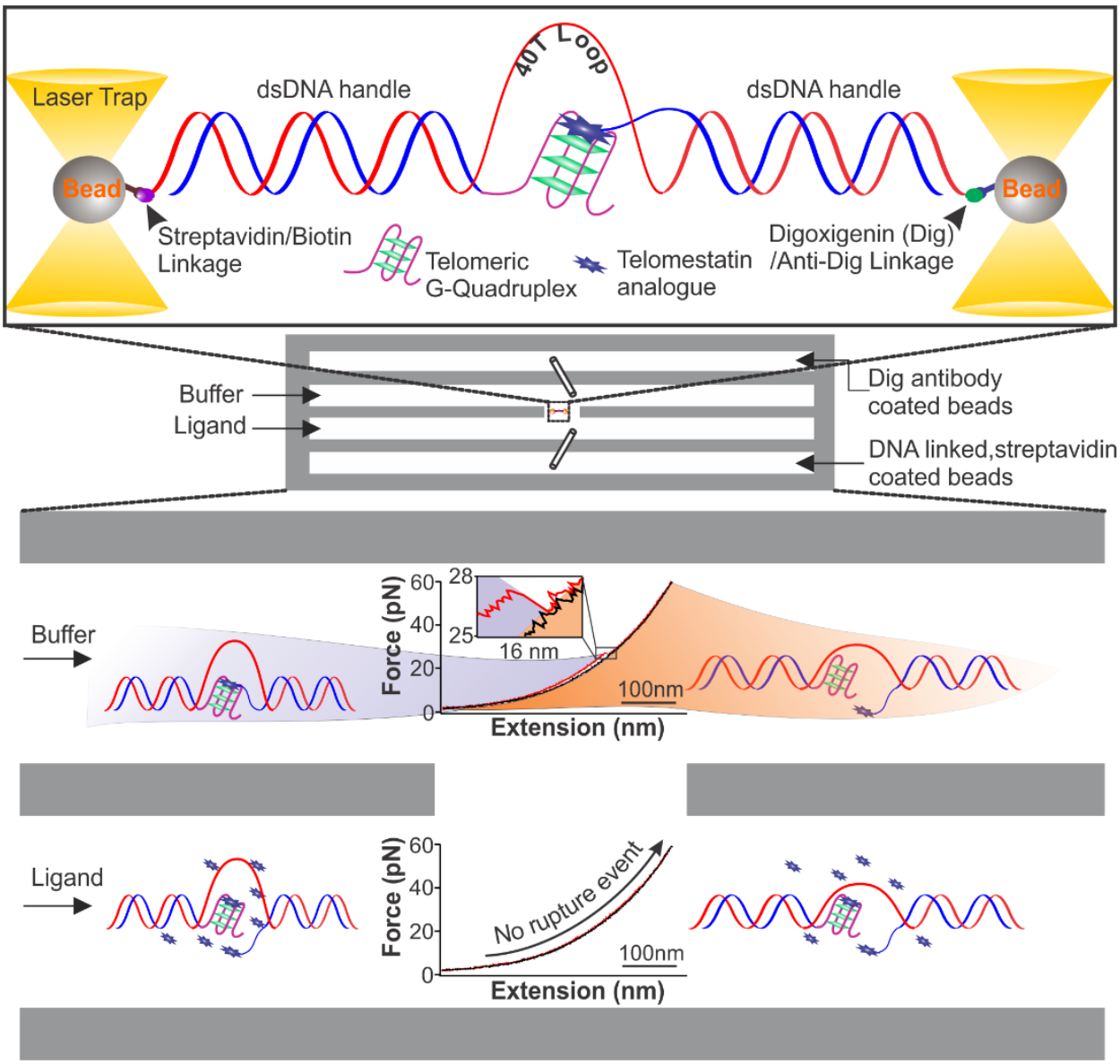

Fig. 1. *Schematic of the single molecule displacement assay. The DNA construct used for the displacement assay is tethered between two beads which are optically trapped. In a buffer channel without free ligand L2H2-6OTD, the G-quadruplex and DNA-tethered L2H2-6OTD are bound. Upon applying a force by pulling the two beads apart, a rupture feature occurs in the force-extension curve (top). In the ligand channel, the DNA-tethered L2H2-6OTD is displaced by the free ligands, which yields an F-X curve that does not contain any rupture features (bottom).*

the preparation procedure since only one type of ligands needs to be labelled to report its displacement. Another advantage of this displacement assay comes from the unique capability of probing small-molecule ligands that otherwise cannot be accomplished by conventional methods which have low sensitivities to small molecules.[33, 34]

However, there exists challenges in the displacement assay at the single molecular level[30, 35] due to immobilization issues as well as the long-term tracking of single fluorophores that are prone to photobleaching.

Here, we invented a single-molecule displacement assay (smDA) in a force-based optical tweezers instrument. Given the importance of G-quadruplex in various sensing devices[36-38] and biological activities[39-44], we used smDA to estimate the K_d between human telomeric DNA G-quadruplexes and G-quadruplex ligands, L2H2-6OTDs. First, we compared smDA-measured K_d of known L2H2-6OTD ligands (Monomer and Dimer) with those obtained from an established method. After establishing the accuracy of the smDA approach, we used it to evaluate the K_d of a new type of dendrimer G-quadruplex ligands (L2H2-6OTD Trimer and Hexamer). Our smDA conveniently confirmed that dendrimer ligands had much increased binding affinity towards human telomeric G-quadruplex likely due to the polyvalent geometry. We also found that the binding affinity of L2H2-6OTD ligands correlated with their inhibitory activities against human telomerase. This single-molecule displacement assay can be utilized to screen different binding molecules. In addition, the finding of effective binding of dendrimer ligands to the DNA G-quadruplex offers new guidelines in the design of G-quadruplex ligands to potentially treat various G-quadruplex associated diseases.

2. Experimental

2.1. Chemicals

All DNA oligonucleotides used in this research were purchased from IDT (Integrated DNA technologies, IA). Their sequences can be found in SI page S33, table 1&S1. Enzymes were purchase from NEB (New England Biolabs, England). Polystyrene beads (streptavidin-coated and anti-digoxigenin antibody-coated) used for trapping in optical tweezers were purchased from Spherotech (Lake Forest, IL). All chemicals and reagents were purchased from Sigma Aldrich or Fisher Scientific, unless otherwise stated, and were used without further purification.

Table 1. Oligonucleotide sequences used to prepare the construct

Oligo name	**Sequence (5’ → 3’)**
4G Oligo (57nts)	CAGGGACGCGCTGGGCTACGTCTTGCTGGCTTTGGGTTAGGGTTAGGGTTAGGGTTA
Oligo 1 (25nts)	/5Hexynyl/GGCTACACTAGAAGGACAGTATTTG
40T-looped oligo (94nts)	CTAGCAAATACTGTCCTTCTAGTGTAGCTTTTTTTTTTTTTTTTTTTTTTTTTTTTTTTTTTTTT TTTGCCAGCAAGACGTAGCCCAGCGCGTC

2.2. Synthesis of single-molecule displacement assay construct

A detailed procedure for the synthesis of single-molecule displacement construct is shown in SI section 5. As shown in Fig. 1, the construct consists of 1558bp and 2391bp dsDNA handles connected with 40T ssDNA loop. In brief, 5' L2H2-6OTD linked Oligo1, Phosphorylated-4G Oligo, and Phosphorylated-40T looped Oligo (Table S1) were annealed at 95°C for 5 mins and cooled to room temperature in 2.5 hours with a temperature ramping rate of 1°C per min. The annealed construct was ligated with 1558bp handle by T4 DNA ligase at 16°C for 16 hours and purified by gel. Finally, the purified 1558bp handle ligated construct was ligated with the 2391bp handles by T4 DNA ligase at 16°C for 16 hours to obtain the final construct for the optical tweezers experiment. The 1558bp handle was labelled with biotin on its 5' end by PCR, while 2391bp was labelled with digoxigenin in its 3' end by terminal transferase and dig-dUTP. Getting DNA tethers between two optically trapped beads in the optical-tweezer instrument indicated that the ligation of both handles was successful.

2.3. *Single molecule displacement assay in optical tweezers*

Single-molecule displacement assays were performed in a dual-trap laser-tweezers instrument. A four channel glass microfluidic chamber was used (see Figure S3). A 10 mM Tris buffer containing 100 mM KCl at pH 7.4 (23 °C) was used throughout the experiment. From the top channel, polystyrene beads coated with anti-digoxigenin antibody were flowed in. Beads coated with smDA construct were flowed into the bottom channel. In the middle two channels, ligand and buffer were flowed from top and bottom channels, respectively. The two beads from top and bottom channels were captured at laser foci separately and the smDA construct was tethered between the two trapped beads by bringing the beads close to each other. Upon moving two beads apart, the tethered DNA was stretched, and the tension exerted on the G-quadruplex – ligand complex was calculated. The resulting force-extension (F-X) curves were recorded through LabView program (National Instruments, Austin, TX) at 1KHz with loading rate of 5.5 pN/s (in the 10-30 pN force range). A detailed procedure for performing smDA in optical tweezers can be found in SI section 3.

3. Results and discussion

3.1. Force based single-molecule displacement assay

In a displacement assay, it is required to form a ligand-receptor complex to be displaced by other ligand molecules. Here we used a human telomeric DNA G-quadruplex and a telomestatin analogue, L2H2-6OTD[45, 46], as an exemplary binding complex (Fig. 1). We covalently attached the L2H2-6OTD to the end of a DNA strand (see SI Fig. S1) while

placing the G-quadruplex forming sequence, 5'-$(TTAGGG)_4TTA$, on the end of another DNA strand. These two DNA strands were hybridized separately into a DNA template (Fig. 1, see SI Fig. S4) in such a way that the G-quadruplex and the L2H2-6OTD were facing each other to facilitate the so-called cognate binding[47]. The distance of these two binding components was controlled by a T_{40} loop. Such a strategy[48] allowed the close distance between the G-quadruplex and L2H2-6OTD even when they were dissociated. The close distance then facilitated the rebinding of the two dissociated components, increasing the throughput of repetitive binding/dissociation processes.

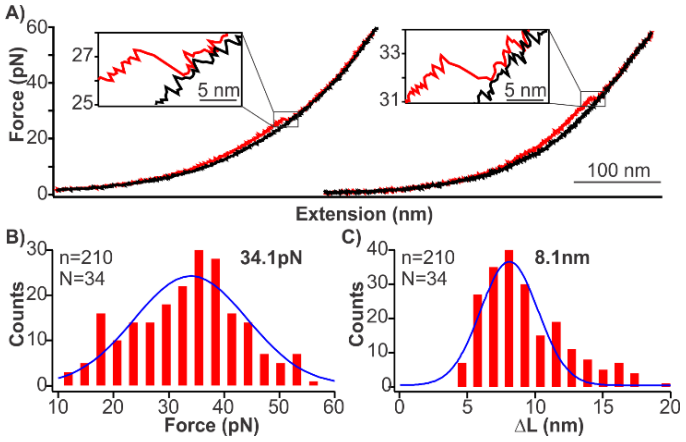

Fig. 2. *Unfolding features of the binding complex between telomere G-quadruplex and L2H2-6OTD ligand. A) Two typical F-X curves obtained after mechanical pulling of the construct in optical tweezers. Red and black curves depict the stretching and relaxing processes, respectively. B) Rupture force and C) change-in-contour-length histograms obtained from the rupture features in A). The Gaussian center for the rupture force is 34.1 pN and that for ΔL is 8.1 nm (average 10.1 nm). The blue curves in the histograms are Gaussian fittings. N and n represent the total molecules and total features, respectively.*

We first investigated mechanical features of the rupture events between the L2H2-6OTD and telomeric G-quadruplex binding complex. As shown in Fig. 1, the two dsDNA handles were tethered to two optically trapped beads by affinity linkages of the streptavidin-biotin and digoxigenin(dig) – dig antibody complexes, respectively. To start each experiment, two optically trapped beads were moved apart by a steerable mirror that controlled one of the two trapping lasers in the optical-tweezers instrument. The departure of the two trapped beads increased the tensile force in the DNA construct, which allowed the mechanical unbinding of the L2H2-6OTD – G-quadruplex complex (Fig. 2A). Plotting of the unbinding force histogram gave a mechanical force centered at 34.1 pN (Fig. 2B). It is significant that the mechanical stability of the G-quadruplex – L2H2-6OTD complex was higher than that of the telomeric G-quadruplex unfolded from the 5' and 3' ends (~20 pN)[49], but lower than that of the L2H2-6OTD bound G-quadruplex disassembled from the 5' and 3' ends (37 pN)[50]. Although it is not clear whether the G-quadruplex structure was intact during the rupture of the binding complex. The rupture event accompanied with a change-in-contour-length (ΔL) of

8.1 nm (Gaussian center, average is 10.1±3.6 nm), which allowed us to identify the dissociation of the G-quadruplex–L2H2-6OTD interaction. It is noteworthy that the change-in-contour-length was a little lower than that expected for the T40 bridge (~12 nm, see SI Fig. S6 for the calculation of the change-in-contour-length), which may reflect an extended geometry between the L2H2-6OTD – G-quadruplex interaction (~3.4 nm GQ overhang and 3.4 nm telomestatin overhang).

With this single-molecule setup, we continued to perform the displacement assay in optical tweezers (Fig. 1). In a solution, free L2H2-6OTD ligands can compete with the DNA-linked L2H2-6OTD to bind to the G-quadruplex. Such a displacement is expected to dissociate the cognate L2H2-6OTD/G-quadruplex complex. As a result, when force is ramped up, no rupture feature should be observed. Therefore, the rupture events in presence of free ligands can be used to indicate whether displacement of DNA-linked ligand has occurred. However, the force-extension curves without any rupture feature does not necessarily mean that there is no interaction between the cognate L2H2-6OTD and G-quadruplex complex. It is possible that their mechanical stability is so strong that the cognate L2H2-6OTD/G-quadruplex pair still remains bound even subjecting to high mechanical forces (~ 60 pN). These non-unfolded curves should shift from the F-X trajectories without any binding complex by a value of ΔL (~10 nm). Therefore, they can be easily identified. By comparing the numbers of the F-X traces with and without unbinding features, we quantified the percentage of free ligand bound G-quadruplex at a particular ligand concentration (see SI Fig. S5 for detailed calculation). This information was then plotted against the free ligand concentration to construct the binding curves of various ligands to the telomeric G-quadruplex.

142 *3.2. Binding of L2H2-6OTD ligands to the DNA telomeric G-quadruplex*

143 To test the accuracy of this smDA method, we performed the displacement experiments using monomeric
144 (Monomer) and dimeric (Dimer) L2H2-6OTD ligands (Fig. 3). Using the procedure described above, we calculated
145 the percentages of the G-quadruplex bound to each ligand at various concentrations (Fig. 3). It is obvious that at high
146 concentrations of free ligands, the displacement of the free ligand to the DNA tethered ligand is more efficient. The
147 resultant binding curve was fit with a Langmuir isotherm (see SI section 12) to obtain K_d (22±3 nM for Monomer and
148 20±3 nM for Dimer). It is expected that the Dimer has increased binding affinity with respect to Monomer due to its

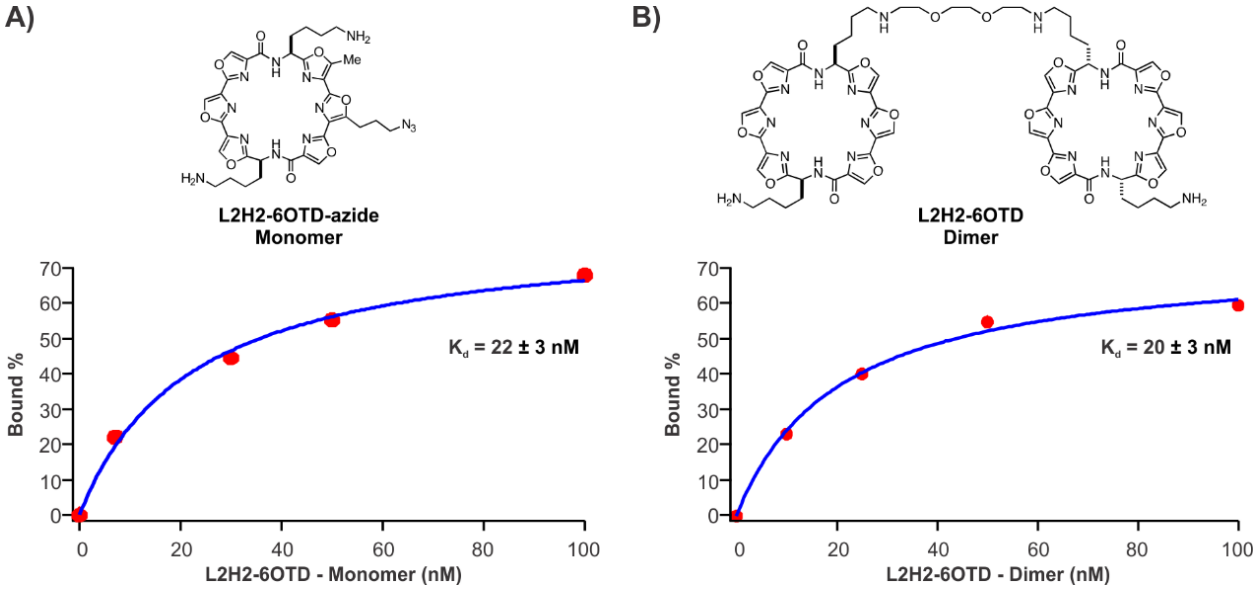

Fig. 3. Binding curves of the Monomer (A) and the Dimer (B) L2H2-6OTD ligands to the telomeric G-quadruplex.

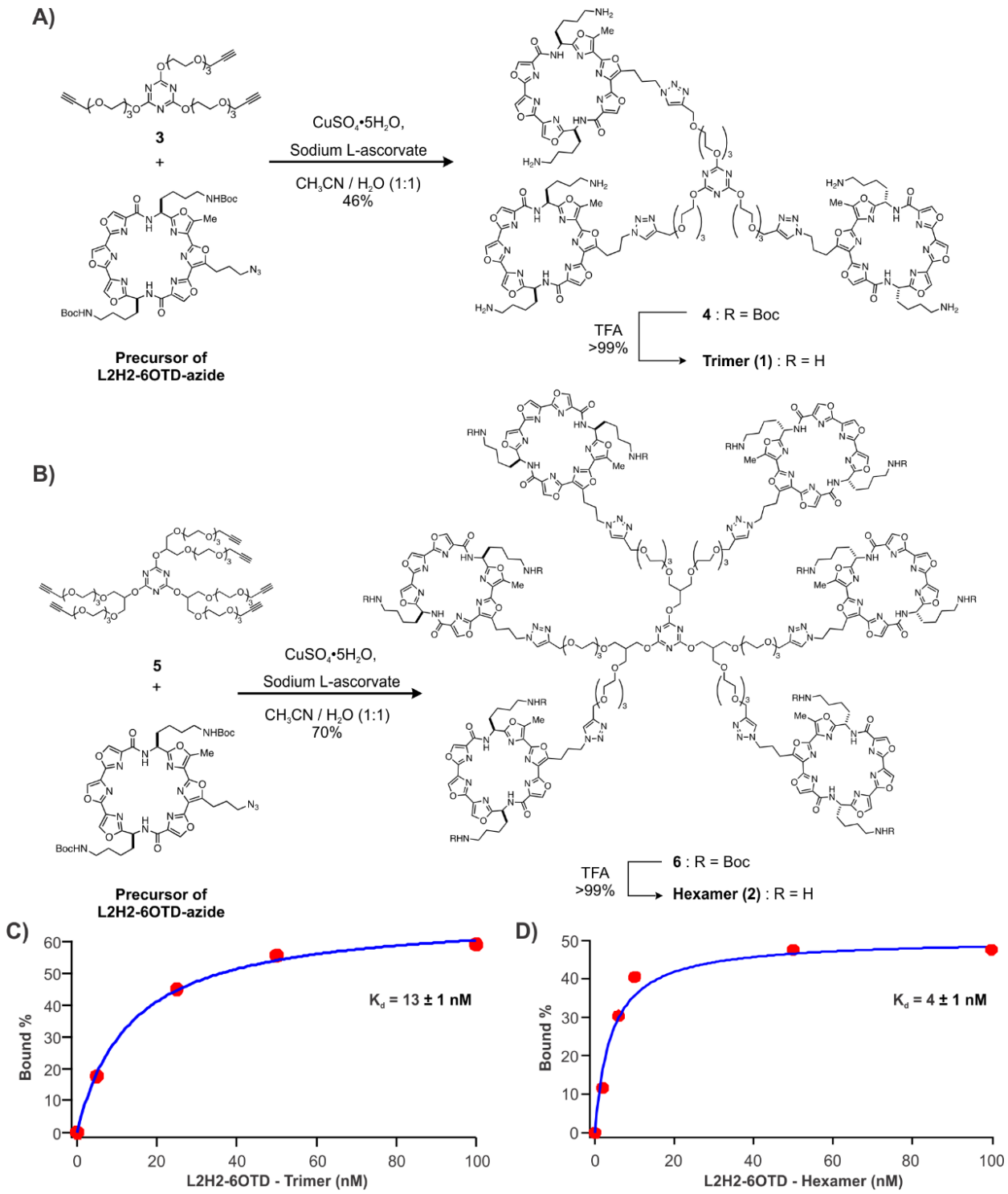

Fig. 4. *Preparation of dendrimer L2H2-6OTD ligands (Trimer (A) and Hexamer (B)). Binding curves of the Trimer (C) and Hexamer (D) ligands to the G-quadruplex revealed by the single-molecule displacement assay.*

149 divalent L2H2-6OTD units.[51] Compared to the K_d measured by ensemble assays (15 nM for Monomer and 8 nM for

150 Dimer)[52] as well as single-molecule methods (14±1 nM for Monomer and 13±1 nM for Dimer),[51] our results showed

similar values given the involvement of different procedures. In previously demonstrated single-molecule measurements, the binding of the ligand to the G-quadruplex was evaluated by increased mechanical stability of the G-quadruplex, which was unfolded by grabbing the 5' and 3' ends. Such a geometry of unfolding may weaken the G-quadruplex structure before its rupture force, compromising the binding of the ligand to the G-quadruplex. As a result, the mechanical stability of the G-quadruplex-ligand complex can be compromised, leading to its mis-assignment to the population of unbound G-quadruplex. In fact, it is quite often that the bound percentage of G-quadruplex was below 40% even at saturated ligand concentrations. This smDA strategy avoided this biased observation, making more accurate identification of free and ligand-bound G-quadruplex populations.

With the establishment of accurate K_d measurement using smDA method, we proceeded to evaluate dendrimer L2H2-6OTD ligands (Trimer and Hexamer) (Fig. 4). We argued that the polyvalent nature of the dendrimer framework[51, 53] should increase the binding affinity of the ligands to the G-quadruplex. To this purpose, we prepared the dendrimer L2H2-6OTD ligands (Trimer **1** and Hexamer **2**) in Fig. 4 (see SI sections 9&10 for detailed syntheses). In short, a dendrimer core **3** [54] and L2H2-6OTD-azide[45] were subjected to a copper catalyzed Huisgen coupling reaction, and the Boc group of the resulting Trimer **4** was deprotected with TFA (trifluoroacetic acid) to give Trimer **1** in 46% yields (two steps). Similarly, Hexamer **2** was synthesized from dendrimer core **5** and L2H2-6OTD azide[45] via Hexamer **6** in 70% yield. Six and twelve TFA molecules served as counter-ions during the syntheses of the Trimer and Hexamer, respectively. The solubility of these compounds was confirmed via HPLC in MilliQ water (10 μM containing 0.1% DMSO). The dendrimer core used here, cyanuric acid, is "essentially nontoxic"[55] and often employed in drinking water and animal feed. Compared to the PAMAM, the most widely used dendrimer that has shown membrane damage of cells due to its positive surface charges,[56, 57] the nontoxic dendrimer core and the biocompatible ethylene glycol framework adopted here are expected to target cancer cells through binding of G-quadruplexes formed in their elongated telomere overhangs without much nonspecific interaction of negatively charged DNA backbones.

Evaluation of the K_d of these two dendrimer ligands using the smDA method revealed K_d values of 13±1 nM and 4±1 nM for the Trimer and Hexamer, respectively. This K_d trend is consistent with known single-molecule experiments based on the mechanical stability of bound complexes (3±1 and 2±1 nM for Trimer and Hexamer, respectively) (manuscript submitted). Apart from the variation of the unfolding geometry between our method and the known method as discussed above, the difference in the K_d measurement can also be attributed to the fact that our displacement assay is based on the competition between dendrimer ligands and the monomer ligands, whereas in the

mechanical unfolding assay, it is the direct measurement of the binding complex between G-quadruplex and specific ligands. Taken together, our results clearly verify the hypothesis that polyvalent dendrimer L2H2-6OTD ligands indeed have better binding affinities than the monomeric (Monomer) or linear (Dimer) ligand (see Fig. 5 for summary).

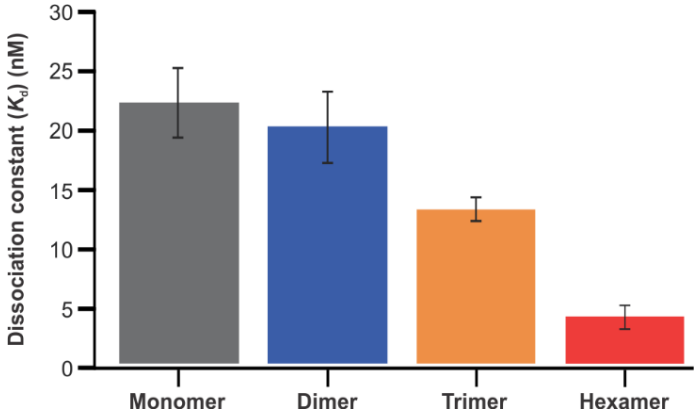

Fig. 5. *Comparison of the dissociation constants (K_d) among the Monomer, Dimer, Trimer, and Hexamer L2H2-6OTD ligands. Error bars represent standard deviations from three independent experiments.*

3.3. Inhibition of telomerase activities by L2H2-6OTD ligands

The polyvalent geometry of the dendrimer ligands led us to propose that these ligands would be ideal for binding with tandem telomeric G-quadruplexes that are also polyvalent.[51] To test this hypothesis, we investigated the inhibitory effects of linear and dendrimer ligands on the telomerase catalyzed elongation of telomeric DNA fragment. Previously, it has been found that G-quadruplex ligands can selectively target 3' telomere overhang and inhibit telomere elongation by telomerase through stabilization of telomeric G-quadruplex.[58, 59] Therefore, by comparing telomerase inhibitory actions of the dendrimer ligands with respect to the monomer or dimer L2H2-6OTD ligand, it can provide support to the hypothesis that polyvalent dendrimer ligands present higher binding affinities with telomeric G-quadruplex. We tested the inhibitory effect of the dendrimer ligands using the TRAP assay[60] in which a DNA primer was elongated with the 5'-GGTTAG repeats by human telomerase. The elongated product was analyzed by PCR amplification. The longer the added telomeric repeats, the higher the activity of the telomerase (Fig. 6). However, artefacts arise since the DNA polymerase used in the PCR amplification is also inhibited by G-quadruplex, which is aggravated by the ligand binding to the G-quadruplex.[61] To minimize these artefacts, we used phenol-chloroform extraction followed by Amicon® filtration to remove the L2H2-6OTD compounds remained in the solution after telomerase catalyzed extensions (see SI section 8).

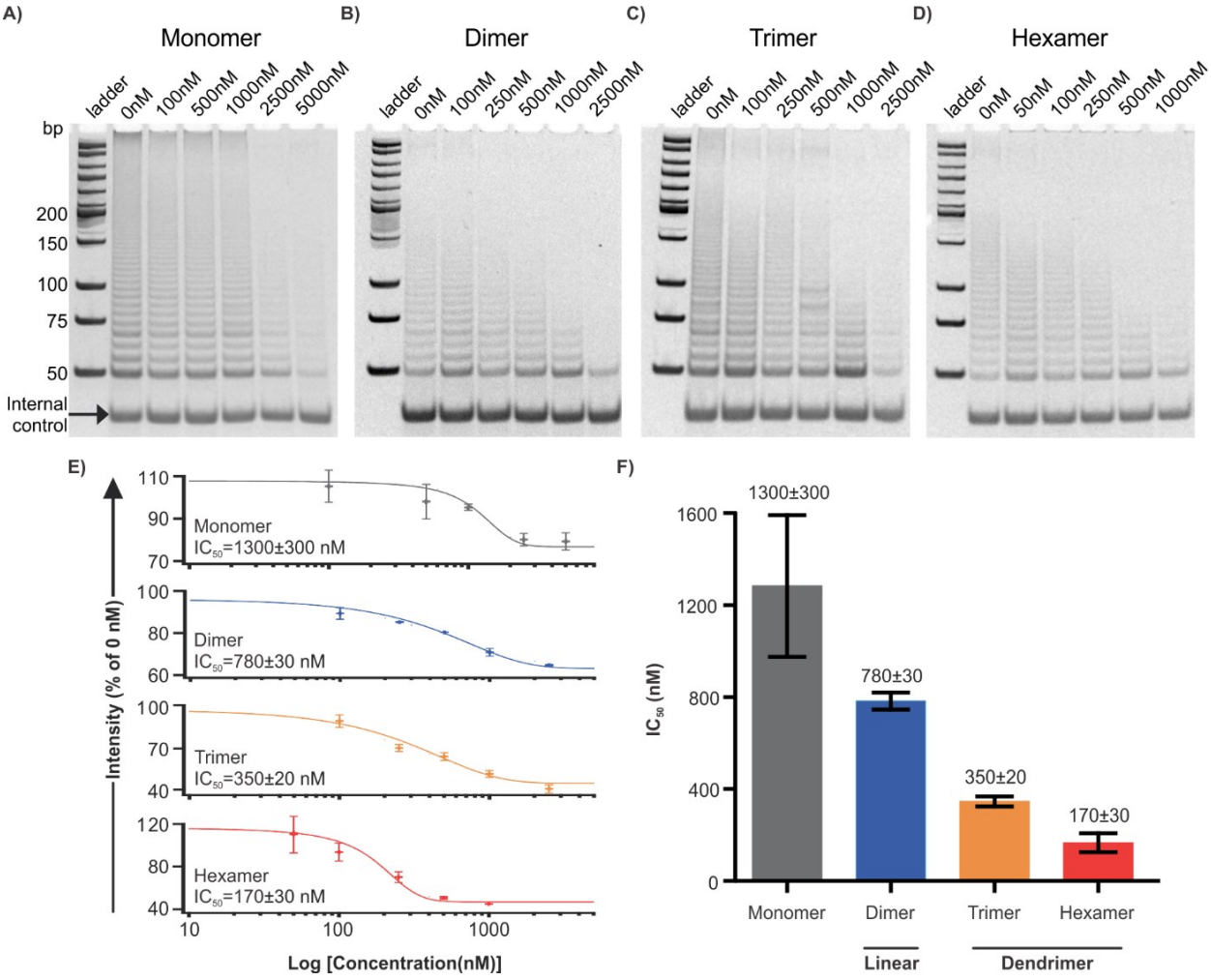

198

Fig. 6. *Inhibition of telomerase activities by L2H2-6OTD compounds. Telomerase activities were tested by the TRAP assay in PAGE gels with various concentrations of L2H2-6OTD Monomer (A, 0-5000 nM), Dimer (B, 0-2500 nM), Trimer (C, 0-2500 nM) and Hexamer (D, 0-1000 nM). Compounds were added during the telomerase mediated elongation to reveal their effects on the elongation. These compounds were then removed by filtration before the PCR amplification of the elongated products, which were detected on 8% native PAGE. The IC_{50} (E, 50% inhibition of telomerase activity, 1300±300 nM for the Monomer, 780±30 nM for the Dimer, 350±20 nM for the Trimer, and 170±30 nM for the Hexamer) was calculated from the intensity of all the bands except the control bands on PAGE gels. The IC_{50} values for all five ligands were shown in the bar histogram (F). Standard deviations (error bars) where calculated from three independent experiments.*

199 After running the gel for the PCR amplified, telomerase elongated products under different concentrations of the
200 L2H2-6OTD ligands (Fig. 6 A-D), we analyzed IC_{50} of the telomerase inhibition among different dendrimer and linear
201 ligands (Fig. 6E). We observed that while dendrimer ligands Hexamer and Trimer represented the top two most potent
202 inhibitions, respectively, the linear ligand Dimer had reduced effects, followed by the Monomer which presented the

lowest inhibitory potency. This order (Fig. 6F) followed well with the ranking of the binding affinities among four ligands (Fig. 5), indicating that it is the binding affinity in L2H2-6OTD ligands that causes the different inhibitory effects against telomerase. The better affinities of dendrimer L2H2-6OTD ligands are likely due to the polyvalent effect derived from the dendrimer framework. These results not only support the smDA finding of increased affinity of dendrimer ligands towards G-quadruplex, but they also provide a new approach to develop G-quadruplex ligands that are instrumental to fight various diseases.

4. Conclusion

In summary, we have invented a new method, single-molecule displacement assay, to evaluate the dissociation constants between L2H2-6OTD ligands and human telomeric G-quadruplex. Compared to previous single-molecule binding measurement that exploits mechanical stability of a binding complex,[51] which can be disruptive to the receptor structure, this method is nonintrusive as receptor structures are not mechanically unfolded. As a result, it provides a more accurate profile for the binding process. In addition, the displacement nature allows a direct comparison of a pre-existing ligand with desired ligands in solution. This facilitates the screening of more effective ligands to a receptor. Using this approach, we found dendrimer G-quadruplex ligands have much increased binding affinity. This dendrimer ligand structure offered a new direction in the design of more effective molecules against DNA G-quadruplex structures, which are involved in many diseases such as cancers.

5. Supplementary data

The Supporting Information is available free of charge on the Analytical Biochemistry Journal website.

Synthesis of L2H2-6OTD modified oligo, synthesis of the construct for single molecule displacement assays, force-extension curves to identify the single molecules, four-channel microfluidic chamber, calculation of ligand bound percentage, calculation of change-in-contour-length, protocol for the TRAP assay, synthesis of Trimer and Hexamer ligands, NMR spectra of the synthetic compounds, fitting the bound % *vs* concentration of ligands with Langmuir model to estimate K_d, and sequences of oligonucleotides used in this study.

6. Acknowledgments

H.M. thanks NIH (R01 CA236350) and NSF (CBET1904921) for financial support.

7. Author's contribution

The manuscript was written through contributions of all authors. † These authors contributed equally.

8. Declaration of competing interests

The authors declare no conflict of interest.

9. References

1. Engvall, E., [28] Enzyme immunoassay ELISA and EMIT. In *Methods in Enzymology*, Academic Press: 1980; Vol. 70, pp 419-439.
2. Khanna, K.; Mandal, S.; Blanchard, A. T.; Tewari, M.; Johnson-Buck, A.; Walter, N. G., Rapid kinetic fingerprinting of single nucleic acid molecules by a FRET-based dynamic nanosensor. *Biosensors and Bioelectronics* **2021,** *190*, 113433.
3. Kaur, A.; Ellison, M.; Dhakal, S., MASH-FRET: A Simplified Approach for Single-Molecule Multiplexing Using FRET. *Analytical Chemistry* **2021,** *93* (25), 8856-8863.
4. Okamoto, K.; Sannohe, Y.; Mashimo, T.; Sugiyama, H.; Terazima, M., G-quadruplex structures of human telomere DNA examined by single molecule FRET and BrG-substitution. *Bioorg. Med. Chem.* **2008,** *16* (14), 6873-6879.
5. Bruns, N.; Pustelny, K.; Bergeron, L. M.; Whitehead, T. A.; Clark, D. S., Mechanical Nanosensor Based on FRET within a Thermosome: Damage-Reporting Polymeric Mater. *Angew. Chem. Int. Ed. Engl.* **2009,** *48*, 5666-5669.
6. Chen, H. H.; Ho, Y. P.; Jiang, X.; Mao, H. Q.; Wang, T. H.; Leong, K. W., Simultaneous Non-invasive Analysis of DNA Condensation and Stability by Two-step QD-FRET. *Nano Today* **2009,** *4* (2), 125-134.
7. Roy, R.; Hohng, S.; Ha, T., A practical guide to single-molecule FRET. *Nat Meth* **2008,** *5* (6), 507-516.
8. Neuman, K. C.; Nagy, A., Single-molecule force spectroscopy: optical tweezers, magnetic tweezers and atomic force microscopy. *Nat Meth* **2008,** *5* (6), 491-505.
9. Amemiya, Y.; Furunaga, Y.; Iida, K.; Tera, M.; Nagasawa, K.; Ikebukuro, K.; Nakamura, C., Analysis of the unbinding force between telomestatin derivatives and human telomeric G-quadruplex by atomic force microscopy. *Chem Comm* **2011,** *47* (26), 7485-7487.
10. Carrion-Vazquez, M.; Marszalek, P. E.; Oberhauser, A. F.; Fernandez, J. M., Atomic force microscopy captures length phenotypes in single proteins. *Proc Natl Acad Sci U S A* **1999,** *96* (20), 11288-92.
11. Fotiadis, D.; Scheuring, S.; Müller, S. A.; Engel, A.; Müller, D. J., Imaging and manipulation of biological structures with the AFM. *Micron* **2002,** *33* (4), 385-397.
12. Karrasch, S.; Hegerl, R.; Hoh, J. H.; Baumeister, W.; Engel, A., Atomic force microscopy produces faithful high-resolution images of protein surfaces in an aqueous environment. *Proc Natl Acad Sci U S A* **1994,** *91* (3), 836-838.
13. Lyubchenko, Y. L., DNA structure and dynamics: an atomic force microscopy study. *Cell Biochem. Biophys.* **2004,** *41*.
14. Peng, Q.; Li, H., Atomic force microscopy reveals parallel mechanical unfolding pathways of T4 lysozyme: Evidence for a kinetic partitioning mechanism *Proc. Nat. Acad. Sci. USA* **2008,** *105*, 1885-1890.
15. Grandbois, M.; Beyer, M.; Rief, M.; Clausen-Schaumann, H.; Gaub, H. E., How Strong Is a Covalent Bond? *Science* **1999,** *283* (5408), 1727-1730.
16. Bockelmann, U.; Thomen, P.; Essevaz-Roulet, B.; Viasnoff, V.; Heslot, F., Unzipping DNA with Optical Tweezers: High Sequence Sensitivity and Force Flips. *Biophys. J.* **2002,** *82*, 1537-1553.
17. Ashkin, A., Optical Trapping and Manipulation of Neutral Particles using Lasers. *Proc. Natl. Acad. Sci. USA* **1997**, 4853-4860.
18. Ashkin, A., History of optical trapping and manipulation of small-neutral particle, atoms, and molecules. *IEEE J. Sel. Topics Quantum Electron.* **2000,** *6*, 841-856.
19. Williams, M. C., Optical tweezers: measuring piconewton forces. *Biophysics Textbook Online: http://www. biophysics. org/btol* **2002**.

20. Wang, M. D.; Yin, H.; Landick, R.; Gelles, J.; Block, S. M., Stretching DNA with optical tweezers. *Biophysical Journal* **1997,** *72* (3), 1335-1346.
21. Gosse, C.; Croquette, V., Magnetic Tweezers: Micromanipulation and Force Measurement at the Molecular Level. *Biophy. J.* **2002,** *82*, 3314-3329.
22. Long, X.; Parks, J. W.; Bagshaw, C. R.; Stone, M. D., Mechanical unfolding of human telomere G-quadruplex DNA probed by integrated fluorescence and magnetic tweezers spectroscopy. *Nucleic Acids Res.* **2013,** *41* (4), 2746-2755.
23. Seol, Y.; Neuman, K. C., Magnetic Tweezers for Single-Molecule Manipulation. In *Single Molecule Analysis: Methods and Protocols*, Peterman, E. J. G.; Wuite, G. J. L., Eds. Humana Press: Totowa, NJ, 2011; pp 265-293.
24. Vilfan, I.; Lipfert, J.; Koster, D.; Lemay, S.; Dekker, N., Magnetic tweezers for single-molecule experiments. In *Handbook of Single-Molecule Biophysics*, Hinterdorfer, P.; Oijen, A., Eds. Springer US: 2009; pp 371-395.
25. Zhang, C.; Fu, H.; Yang, Y.; Zhou, E.; Tan, Z.; You, H.; Zhang, X., The Mechanical Properties of RNA-DNA Hybrid Duplex Stretched by Magnetic Tweezers. *Biophysical Journal* **2019,** *116* (2), 196-204.
26. Koirala, D.; Shrestha, P.; Emura, T.; Hidaka, K.; Mandal, S.; Endo, M.; Sugiyama, H.; Mao, H., Single-molecule mechanochemical sensing using DNA origami nanostructures. *Angew. Chem. Int. Ed. Engl.* **2014,** *53*, 8137-8141.
27. Nguyen, T.-H.; Steinbock, L. J.; Butt, H.-J.; Helm, M.; Berger, R. d., Measuring Single Small Molecule Binding via Rupture Forces of a Split Aptamer. *J. Am. Chem. Soc.* **2011,** *133* (7), 2025-2027.
28. Yangyuoru, P. M.; Dhakal, S.; Yu, Z.; Koirala, D.; Mwongela, S. M.; Mao, H., Single-Molecule Measurements of the Binding between Small Molecules and DNA Aptamers. *Anal. Chem.* **2012,** *84*, 5298-5303.
29. Shrestha, P.; Mandal, S.; Mao, H., Invited Review. Mechanochemical Sensing: A Biomimetic Sensing Strategy. *ChemPhysChem* **2015,** *16* (9), 1829-1837.
30. Wang, X.; Cohen, L.; Wang, J.; Walt, D. R., Competitive Immunoassays for the Detection of Small Molecules Using Single Molecule Arrays. *Journal of the American Chemical Society* **2018,** *140* (51), 18132-18139.
31. Monchaud, D.; Allain, C.; Bertrand, H.; Smargiasso, N.; Rosu, F.; Gabelica, V.; De Cian, A.; Mergny, J. L.; Teulade-Fichou, M. P., Ligands playing musical chairs with G-quadruplex DNA: A rapid and simple displacement assay for identifying selective G-quadruplex binders. *Biochimie* **2008,** *90* (8), 1207-1223.
32. Monchaud, D.; Allain, C.; Teulade-Fichou, M.-P., Development of a fluorescent intercalator displacement assay (G4-FID) for establishing quadruplex-DNA affinity and selectivity of putative ligands. *Bioorganic & Medicinal Chemistry Letters* **2006,** *16* (18), 4842-4845.
33. Mayer, K. M.; Hafner, J. H., Localized surface plasmon resonance sensors. *Chem. Rev.* **2011,** *111* (6), 3828-57.
34. Petryayeva, E.; Krull, U. J., Localized surface plasmon resonance: Nanostructures, bioassays and biosensing—A review. *Analytica Chimica Acta* **2011,** *706* (1), 8-24.
35. Rissin, D. M.; Kan, C. W.; Campbell, T. G.; Howes, S. C.; Fournier, D. R.; Song, L.; Piech, T.; Patel, P. P.; Chang, L.; Rivnak, A. J.; Ferrell, E. P.; Randall, J. D.; Provuncher, G. K.; Walt, D. R.; Duffy, D. C., Single-molecule enzyme-linked immunosorbent assay detects serum proteins at subfemtomolar concentrations. *Nature Biotechnology* **2010,** *28* (6), 595-599.
36. Xi, H.; Juhas, M.; Zhang, Y., G-quadruplex based biosensor: A potential tool for SARS-CoV-2 detection. *Biosens Bioelectron* **2020,** *167*, 112494-112494.
37. He, H.-Z.; Chan, D. S.-H.; Leung, C.-H.; Ma, D.-L., G-quadruplexes for luminescent sensing and logic gates. *Nucleic Acids Res.* **2013,** *41* (8), 4345-4359.
38. Ruttkay-Nedecky, B.; Kudr, J.; Nejdl, L.; Maskova, D.; Kizek, R.; Adam, V., G-quadruplexes as sensing probes. *Molecules* **2013,** *18* (12), 14760-14779.
39. Han, H.; Hurley, L. H., G-quadruplex DNA: a potential target for anti-cancer drug design. *Trends Pharmacol Sci* **2000,** *21* (4), 136-142.
40. Mergny, J.-L.; Helene, C., G-quadruplex DNA: A target for drug design. *Nat Med* **1998,** *4* (12), 1366-1367.
41. Rhodes, D.; Lipps, H. J., G-quadruplexes and their regulatory roles in biology. *Nucleic Acids Res.* **2015,** *43* (18), 8627-8637.
42. Bochman, M. L.; Paeschke, K.; Zakian, V. A., DNA secondary structures: stability and function of G-quadruplex structures. *Nature Rev Genet* **2012,** *13* (11), 770-780.
43. Cammas, A.; Millevoi, S., RNA G-quadruplexes: emerging mechanisms in disease. *Nucleic Acids Res* **2017,** *45* (4), 1584-1595.
44. Hansel-Hertsch, R.; Di Antonio, M.; Balasubramanian, S., DNA G-quadruplexes in the human genome: detection, functions and therapeutic potential. *Nat Rev Mol Cell Biol* **2017,** *18* (5), 279-284.

45. Punnoose, J. A.; Ma, Y.; Hoque, M. E.; Cui, Y.; Sasaki, S.; Guo, A. H.; Nagasawa, K.; Mao, H., Random Formation of G-Quadruplexes in the Full-Length Human Telomere Overhangs Leads to a Kinetic Folding Pattern with Targetable Vacant G-Tracts. *Biochemistry* **2018**.
46. Tera, M.; Ishizuka, H.; Takagi, M.; Suganuma, M.; Shin-ya, K.; Nagasawa, K., Macrocyclic Hexaoxazoles as Sequence- and Mode-Selective G-Quadruplex Binders. *Angewandte Chemie International Edition* **2008,** *47* (30), 5557-5560.
47. Al-Zyoud, W. A.; Hynson, R. M. G.; Ganuelas, L. A.; Coster, A. C. F.; Duff, A. P.; Baker, M. A. B.; Stewart, A. G.; Giannoulatou, E.; Ho, J. W. K.; Gaus, K.; Liu, D.; Lee, L. K.; Böcking, T., Binding of transcription factor GabR to DNA requires recognition of DNA shape at a location distinct from its cognate binding site. *Nucleic acids research* **2016,** *44* (3), 1411-1420.
48. Pandey, S.; Kankanamalage, D. V. W.; Zhou, X.; Hu, C.; Isaacs, L.; Jayawickramarajah, J.; Mao, H., Chaperone-Assisted Host–Guest Interactions Revealed by Single-Molecule Force Spectroscopy. *Journal of the American Chemical Society* **2019,** *141* (46), 18385-18389.
49. Koirala, D.; Dhakal, S.; Ashbridge, B.; Sannohe, Y.; Rodriguez, R.; Sugiyama, H.; Balasubramanian, S.; Mao, H., A Single-Molecule Platform for Investigation of Interactions between G-quadruplexes and Small-Molecule Ligands. *Nat. Chem.* **2011,** *3*, 782-787.
50. Ghimire, C.; Park, S.; Iida, K.; Yangyuoru, P.; Otomo, H.; Yu, Z.; Nagasawa, K.; Sugiyama, H.; Mao, H., Direct Quantification of Loop Interaction and π–π Stacking for G-Quadruplex Stability at the Submolecular Level. *J. Am. Chem. Soc.* **2014,** *136* (44), 15537-15544.
51. Punnoose, J. A.; Ma, Y.; Li, Y.; Sakuma, M.; Mandal, S.; Nagasawa, K.; Mao, H., Adaptive and Specific Recognition of Telomeric G-Quadruplexes via Polyvalency Induced Unstacking of Binding Units. *J. Am. Chem. Soc.* **2017,** *139*, 7476-7484.
52. Iida, K.; Majima, S.; Nakamura, T.; Seimiya, H.; Nagasawa, K., Evaluation of the Interaction between Long Telomeric DNA and Macrocyclic Hexaoxazole (6OTD) Dimer of a G-quadruplex Ligand. *Molecules* **2013,** *18* (4), 4328-4341.
53. Mammen, M.; Choi, S.-K.; Whitesides, G. M., Polyvalent interactions in biological systems: implications for design and use of multivalent ligands and inhibitors. *Angew. Chem. Int. Ed. Engl.* **1998,** *37*, 2754-2794.
54. Piron, F.; Oprea, C.; Cismaş, C.; Terec, A.; Roncali, J.; Grosu, I., Synthesis of Podands with Cyanurate or Isocyanurate Cores and Terminal Triple Bonds. *Synthesis* **2010,** *10*, 1639-1644.
55. Huthmacher, K.; Most, D., Cyanuric Acid and Cyanuric Chloride. In *Ullmann's Encyclopedia of Industrial Chemistry*.
56. Rittner, K.; Benavente, A.; Bompard-Sorlet, A.; Heitz, F.; Divita, G.; Brasseur, R.; Jacobs, E., New basic membrane-destabilizing peptides for plasmid-based gene delivery in vitro and in vivo. *Molecular therapy : the journal of the American Society of Gene Therapy* **2002,** *5* (2), 104-14.
57. Duncan, R.; Izzo, L., Dendrimer biocompatibility and toxicity. *Advanced drug delivery reviews* **2005,** *57* (15), 2215-37.
58. Sun, D.; Thompson, B.; Cathers, B. E.; Salazar, M.; Kerwin, S. M.; Trent, J. O.; Jenkins, T. C.; Neidle, S.; Hurley, L. H., Inhibition of Human Telomerase by a G-Quadruplex-Interactive Compound. *J Med Chem* **1997,** *40*, 2113-2116.
59. Burger, A. M.; Dai, F. P.; Schultes, C. M.; Reszka, A. P.; Moore, M. J.; Double, J. A.; Neidle, S., The G-quadruplex-interactive molecule BRACO-19 inhibits tumor growth, consistent with telomere targeting and interference with telomerase function. *Cancer Res* **2005,** *65* (4), 1489-1496.
60. Kim, N. W.; Piatyszek, M. A.; Prowse, K. R.; Harley, C. B.; West, M. D.; Peter, L. C. H.; Coviello, G. M.; Wright, W. E.; Weinrich, S. L.; Shay, J. W., Specific Association of Human Telomerase Activity with Immortal Cells and Cancer. *Science* **1994,** *266* (5193), 2011-2015.
61. Mergny, J.-L.; Lacroix, L.; Teulade-Fichou, M.-P.; Hounsou, C.; Guittat, L.; Hoarau, M.; Arimondo, P. B.; Vigneron, J.-P.; Lehn, J.-M.; Riou, J.-F.; Garestier, T.; Hélène, C., Telomerase inhibitors based on quadruplex ligands selected by a fluorescence assay. *Proceedings of the National Academy of Sciences* **2001,** *98* (6), 3062.